[20] J.D. Terwilliger, J. Ott, Linkage Disequilibrium Between Alleles at Marker Loci, Johns Hopkins University Press, Baltomore, 1994.
[21] B. Burwinkel, H.D. Bakker, E. Herschkoviz, S.W. Moses, Y.S. Shin, M.W. Killian, Mutation in liver glycogen phosphorylase gene (*PYGL*) underlying Glycogenosis type IV (Hers disease), Am. J. Hum. Genet. 62 (1998) 785–791.
[22] S. Chang, M.J. Rosenberg, H. Morton, C.A. Francomano, L.G. Biesecker, Identification of a mutation in liver glycogen phosphorylase in glycogen storage disease type IV, Hum. Mol. Genet. 7 (5) (1998) 865–870.
[23] J.W. Hudson, G.B. Golding, M.M. Crerar, Evolution of allosteric control in glycogen phosphorylase, J. Mol. Biol. 234 (1993) 700–721.
[24] B. Lederer, van F. Hoof, van den G. Berghe, H.G. Hers, Glycogen phosphorylase and its converter enzymes in haemolysates of normal human subjects and of patirnts with type VI glycogen storage dosease, Biochem. J. 147 (1975) 23–35.
[25] I. Marie, C. Baussan, N. Moatti, M. Mathieu, A. Lemonnier, Biochemical diagnosis of hepatic glycogen storage diseases: 20 years French experience, Clin. Biochem. 24 (1991) 169–178.
[26] N. Dahan, C. Baussan, N. Moatti, A. Lemonnier, Use of platelets, mononuclear and polymorphonuclear cells in the diagnosis of glycogen storage disease type IV, J. Inher. Metab. Dis. 11 (1988) 253–260.

ELSEVIER

Brain & Development 26 (2004) 57–60

BRAIN & DEVELOPMENT
Official Journal of the Japanese Society of Child Neurology

www.elsevier.com/locate/braindev

Case report

Pyruvate dehydrogenase E1α subunit deficiency in a female patient: evidence of antenatal origin of brain damage and possible etiology of infantile spasms

Naoko Wada[a], Toyojiro Matsuishi[a], Michiko Nonaka[b], Etsuo Naito[c], Makoto Yoshino[a,*]

[a]*Department of Pediatrics and Child Health, Kurume University School of Medicine, 67 Asahi-machi, Kurume, 830-0011, Japan*
[b]*Neonatal Intensive Care Unit, St. Mary's Hospital, Kurume, Japan*
[c]*Department of Pediatrics, School of Medicine, University of Tokushima, Tokushima, Japan*

Received 21 May 2002; received in revised form 30 January 2003; accepted 18 March 2003

Abstract

Enlargement of the lateral ventricles and atrophy of the brain were documented ultrasonographically in utero at as early as 28th week of gestation in a female patient with lactic acidosis due to deficiency of the pyruvate dehydrogenase E1α subunit, demonstrating that the changes characteristic of this disease can occur antenatally. The mechanism of infantile spasms in this disease may be linked to mosaicism of the brain cells involving the normal enzyme and the mutant enzyme.

Keywords: Pyruvate dehydrogenase; E1α deficiency; Antenatal brain damage; Infantile spasms

1. Introduction

Pyruvate dehydrogenase complex (PDHC) is an enzyme complex consisting of five enzymes. The first enzyme of the complex, pyruvate dehydrogenase (E1), is a tetramer consisting of two α-subunits and two β-subunits. A deficiency of α-subunit (E1α) is the most common cause of congenital PDHC deficiency with lactic acidemia [1]. The α subunit gene locus is assigned to Xp22.1 [2]; and accordingly, this gene is subjected to random inactivation. E1α deficiency is often associated with various types of brain damage and neurological symptoms [3], and, notably, a significant difference has been shown in symptoms between female and male patients; and infantile spasms have been encountered almost exclusively in female patients. The antenatal origin of such brain damage has been suspected [4–6], but no supportive evidence has yet been found. Mutations in the gene encoding the α-subunit have been documented in patients with E1α deficiency. We herein report a female patient with E1α deficiency who developed infantile spasms, and in whom anomalous development of the brain was antenatally demonstrated.

2. Case report

This female patient was born after 40 weeks of uncomplicated pregnancy to healthy nonconsanguineous parents. The birth weight was 2020 g. A routine ultrasonographic study performed at the 28th week of gestation showed enlargement of the lateral ventricles of the fetus. A similar finding was noted at the 32nd week of gestation (Fig. 1A). Due to early detection of this enlargement, the baby was transferred to a neonatal intensive care unit immediately after birth. Laboratory findings at this time indicated metabolic acidosis and hyperammonemia (151 μmol/l). Auditory-evoked brainstem response was negative. Elevated concentrations of lactic acid (5.8 mmol/l) and pyruvic acid (0.6 mmol/l) in blood were first found at the age of 70 days. The karyotype of the patient was 46, XX. At the age of 6 months, she developed tonic seizures with series formation, which was diagnosed as infantile spasms. An electroencephalographic tracing taken at this time showed modified hypsarrythmia. Because the

* Corresponding author. Tel.: +81-942-31-7565; fax: +81-942-38-1792.
E-mail address: yoshino@med.kurume-u.ac.jp (M. Yoshino).

0387-7604/03/$ - see front matter © 2003 Elsevier B.V. All rights reserved.
doi:10.1016/S0387-7604(03)00072-X

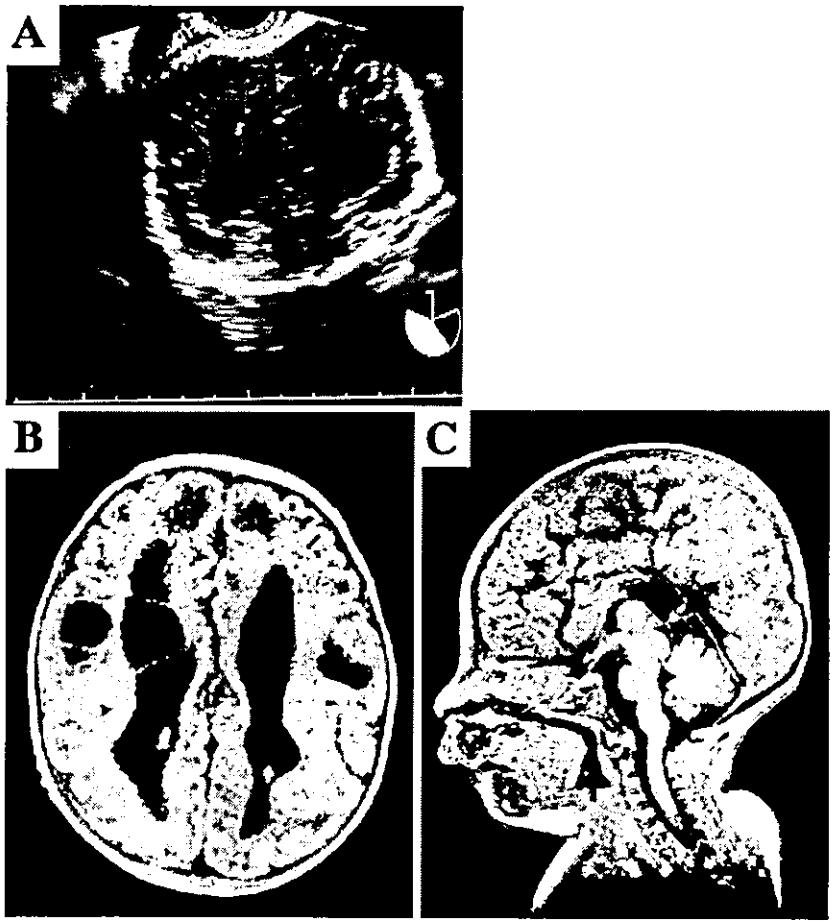

Fig. 1. Enlargement of the lateral ventricles of the fetus was reconfirmed by ultrasonography at the 32nd week of gestation (A). T1-weighted magnetic resonance imaging of the brain recorded at 1 month of age revealed atrophic change of the cerebrum with multiple cystic changes in the brain substance, formation of the intraventricular septum, enlargement of the posterior horns of the lateral ventricles (B), atrophy of the brainstem, and partial agenesis of the corpus callosum (C).

seizure was refractory to vitamin B6, the patient was hospitalized at the age of 6 months for evaluation and management of the seizure. Physical examination on admission revealed a female infant with microcephaly, facial dysmorphism; frontal bossing, laterally upslanting palpebral fissures, depressed nasal bridge, short upturned nose and shark mouth. She had achieved virtually no psychomotor development and had moderate generalized hypotonia with trunkal predominance. The laboratory tests revealed elevated blood concentrations of lactic acid (5.5 mmol/l) and pyruvic acid (0.6 mmol/l), and elevated alanine (1.2 mmol/l) and proline (0.44 mmol/l) levels in serum. Presumptive diagnosis of PDHC E1α deficiency was made at this time. The seizure was ameliorated by the administration of sodium valproate and clonazepam, and the patient was subsequently discharged.

Thiamine hydrochloride at a dose of 10 mg/kg/day was started at the age of 8 months. The patient was readmitted at the age of 11 months, when elevated concentrations of lactic acid (6.2 mmol/l) and pyruvic acid (0.6 mmol/l) in cerebrospinal fluid were found, for the further evaluation. At the age of 13 months, the patient was placed on a high-fat formula. At 16 months of age, after diagnosis had been confirmed by enzyme measurements, administration of sodium dichloroacetate (DCA) was started and maintained at a dose of 50 mg/kg/day for the first 3 months, then tapered to 25 mg/kg/day later (DCA administration had been withheld per parental request until the diagnosis had been confirmed by enzyme analysis). The concentrations of lactic acid and pyruvic acid in blood decreased, with marked fluctuations, shortly after the introduction of DCA and have remained at levels approximately half the pretreatment values. The pretreatment concentrations of lactic acid and pyruvic acid in cerebrospinal fluid were close to those in the blood, and the former levels decreased to approximately two-thirds the pretreatment value 7 days after the initiation of DCA. Nevertheless, no changes in clinical signs have occurred since the introduction of the therapy.

The cranial computerized tomographic (CT) scan on the first day of life showed multiple leukomalacia and enlargement of the lateral ventricles with irregularity of the ventricular walls (figure not shown). Cranial magnetic resonance imaging, first performed at the age of 1 month, revealed, in addition to essentially the same findings as those shown in the previous CT scan, atrophic change of the cerebrum with multiple cystic changes in the brain substance, formations of the intraventricular septum, enlargement of posterior horns of the lateral ventricles (Fig. 1B), atrophy of the brainstem and partial agenesis of corpus callosum (Fig. 1C). The enlargement of the ventricles and atrophic changes of the cerebrum became more marked on the follow-up imagings performed at the ages of 6, 12, and 14 months (figures not shown), irrespective of treatment.

The overall activity (unit, nmol/min/mg protein) of DCA-activated PDHC in cultured skin fibroblasts, measured as described elsewhere [7], was moderately decreased; 0.75 (control range, 2.38 ± 0.60) in the presence of 0.4 mmol/l thiamine pyrophosphate, and 0.53 (control range, 2.31 ± 0.62) in the presence of 1×10^{-4} mmol/l thiamine pyrophosphate. The DCA-activated activity (unit, nmol/h/mg protein) of E1 was 0.69 (control range, 10.7 ± 4.0). Mutational analysis of the E1α gene of the present patient, performed as previously described [7], revealed a deletion of one of the seven base-pair (AGTAAGA) segments of the tandem repeat (nt positions 927–940) in exon 10, creating a termination codon downstream of the deleted segment (nt positions 974–976 in the wild-type sequence).

3. Discussion

It has been postulated that in female patients with E1α deficiency, structural anomalies and degenerative changes in the brain would occur antenatally [4–6]. Observations in our case first demonstrate this postulation, and then confirm that significant retardation of fetal brain development occurs as early as the end of the second trimester in this disease. Additional damage to the brain would be superimposed between that time and delivery because development of the fetal brain becomes more dependent on PDH E1α activity after the mid-organogenesis stage [8]. These observations also suggest that postnatal intervention alone is of limited therapeutic effect. This disease should be included as a differential diagnosis when dilatation of the lateral ventricles is found antenatally.

Scrutiny of clinical records of patients with E1α deficiency [3] revealed that male patients who survived the neonatal period and early infancy generally have a milder phenotype, including mental retardation, ataxia and mild carbohydrate-sensitive lactic acidemia, than female patients, who usually present with seizures, severe developmental delay and structural abnormality of the central nervous system. This observation seems inconsistent with a general rule that in most X-linked dominant diseases, hemizygous male patients usually have a more severe phenotype than heterozygous female patients. A possible explanation for this apparent discrepancy may be as follows. Males who carry a mutant E1α allele that leads to severe deficiency of the enzyme are selected antenatally, and consequently male patients who harbor a mutant E1α allele that results in a less severe enzyme deficiency survive the neonatal period and present as male patients with a mild phenotype. In females, on the other hand, possession of a mutant allele leading to severe enzyme deficiency could still be consistent with a live birth, depending on a pattern of X-inactivation; such individuals would then present a more severe phenotype than male patients who have the mild phenotype.

The pathogenesis of infantile spasms is variable. Neuropathological findings reported in infantile spasms include gross developmental malformations, such as agenesis of the corpus callosum and multifocal dysplastic lesions [9]. The latter is considered to have particular relevance to the mechanism of infantile spasms [10,11]. These cerebral lesions have been observed almost exclusively in female patients with E1α deficiency [3,4], with the exception of one male patient [3]. The vast majority of patients presenting with infantile spasms have been female [12,13]. The presence of such multiple lesions may be linked in part to the pathogenesis of infantile spasms in this disease.

The mosaicism of brain cells may have an implication also in terms of the therapeutic effect of DCA. DCA may not be meaningful in improving pyruvate oxidation in the mutant cells, although it may be effective in reducing the lactic acid released from mutant cells through activation of the enzyme in normal cells. Thus, DCA may have limited therapeutic effect on brain metabolism in female patients.

The seven-base-pair deletion in exon 10 has been reported in multiple patients [14,15]. Clinical presentation among those patients, including the present one, was variable. Though both the nature of mutation and the pattern of the lyonization may affect the phenotype, the former seems to have a more significant influence, as this particular mutation would result in a severe impairment of cellular function in half of the cells of the central nervous system; this is because the mutation is expected to express null activity of the enzyme, given that the wild-type allele and the mutant allele are equally inactivated.

Acknowledgements

This work was supported in part by a grant from the Ministry of Education, Culture, Sports, Sciences and Technology of Japan (No. 12670796). We thank Dr M. Ito (Department of Pediatrics, School of Medicine, University of Tokushima) for the determinations of DCA concentrations; and Drs F. Koga (Neonatal Intensive Care Unit, St. Mary's Hospital), and S. Yoshizawa and S. Nakagawa

(Department of Pediatrics, Kurume University School of Medicine) for their help in patient care and data collection.

References

[1] Dahl HM. Pyruvate dehydrogenase E1α deficiency: males and females differ yet again. Am J Hum Genet 1995;56:553–7.
[2] Brown RM, Dahl HM, Brown GK. X-chromosome localization of the functional gene for the E1 alpha subunit of the human pyruvate dehydrogenase complex. Genomics 1989;4:174–81.
[3] Robinson BH, MacMillan H, Petrova-Benedict R, Sherwood WG. Variable clinical presentation in patients with defective E_1 component of pyruvate dehydrogenase complex. J Pediatr 1987;111:525–33.
[4] Chow CW, Anderson RM, Kenny GCT. Neuropathology in cerebral lactic acidosis. Acta Neuropathol (Berl) 1987;74:393–6.
[5] Michotte A, De-Meirleir L, Lissens W, Denis R, Wayenberg JL, Liebaers I, et al. Neuropathological findings of a patient with pyruvate dehydrogenase E1α deficiency presenting as a cerebral lactic acidosis. Acta Neuropathol 1993;85:674–8.
[6] Takahashi S, Oki J, Miyamoto A, Tokumitsu A, Obata M, Ogawa K, et al. Autopsy findings in pyruvate dehydrogenase E1α deficiency: case report. J Child Neurol 1997;12:519–24.
[7] Naito E, Ito M, Takeda E, Yokota I, Yoshijima S, Kuroda Y. Molecular analysis of abnormal pyruvate dehydrogenase in a patient with thiamine-responsive congenital lactic acidemia. Pediatr Res 1994;36:340–6.
[8] Takakubo F, Dahl HM. Analysis of pyruvate dehydrogenase expression in embryonic mouse brain: localization and developmental regulation. Dev Brain Res 1994;77:63–76.
[9] Jellinger K. Neuropathological aspects of infantile spasms. Brain Dev 1987;9:349–57.
[10] Meencke HJ, Gerhard C. Morphological aspects of aetiology and the course of infantile spasms (West syndrome). Neuropediatrics 1985; 16:59–66.
[11] Chugani HT, Shields WD, Shewmon DA, Olson DM, Phelps ME, Peacock WJ. Infantile spasms: I. PET identifies focal cortical dysgenesis in cryptogenic cases for surgical treatment. Ann Neurol 1990;27:406–13.
[12] Naito E, Ito M, Yokota I, Saijo T, Chen S, Maehara M, et al. Concomitant administration of sodium dichloroacetate and thiamine in west syndrome caused by thiamine-responsive pyruvate dehydrogenase complex deficiency. J Neurol Sci 1999;171:56–9.
[13] Naito E, Ito M, Yokota I, Saijo T, Matsuda J, Ogawa Y, et al. Clinicobiochemical findings of patients with pyruvate dehydrogenase complex deficiency associated with West syndrome. Nihon Shounika Gakkai Zasshi 2000;104:341–5. (in Japanese, with English abstract).
[14] Dahl HM, Maragos C, Brown RM, Hansen LL, Brown GK. Pyruvate dehydrogenase deficiency caused by deletion of a 7-bp repeat sequence in the E1α gene. Am J Hum Genet 1990;47:286–93.
[15] Chun K, MacKay N, Petrova-Benedict R, Federico A, Fois A, Cole DEC, et al. Mutations in the X-linked $E_1\alpha$ subunit of pyruvate dehydrogenase: exon skipping, insertion of duplicate sequence, and missense mutations leading to the deficiency of the pyruvate dehydrogenase complex. Am J Hum Genet 1995;56:558–69.

Journal of Neuroscience Research 77:507–516 (2004)

Genetic Background Markedly Influences Vulnerability of the Hippocampal Neuronal Organization in the "*Twitcher*" Mouse Model of Globoid Cell Leukodystrophy

Kumiko Tominaga,[1] Junko Matsuda,[1]* Makiko Kido,[1] Etsuo Naito,[1] Ichiro Yokota,[1] Kazunori Toida,[2] Kazunori Ishimura,[2] Kunihiko Suzuki,[3] and Yasuhiro Kuroda[1]

[1]Department of Pediatrics, University of Tokushima School of Medicine, Tokushima, Japan
[2]Department of Anatomy and Cell Biology, University of Tokushima School of Medicine, Tokushima, Japan
[3]Institute of Glycotechnology, Future Science and Technology Joint Research Center, Tokai University, Hiratsuka, Japan

The *twitcher* mouse is well known as a naturally occurring authentic mouse model of human globoid cell leukodystrophy (GLD; Krabbe disease) due to genetic deficiency of lysosomal galactosylceramidase. The *twitcher* mice used most commonly are on the C57BL/6J background. We generated *twitcher* mice that were on the mixed background of C57BL/6J and 129SvEv, the standard strain for production of targeted mutations. *Twitcher* mice on the mixed background were smaller and had a shorter lifespan than were those on the C57BL/6J background. Many *twitcher* mice on the mixed background developed generalized seizures around 30 days that were never seen in *twitcher* mice on the C57BL/6J background. Neuropathologically, although the degree of the typical demyelination with infiltration of macrophages was similar in the central and peripheral nervous systems, in both strains, marked neuronal cell death was observed only in *twitcher* mice on the mixed background. In the hippocampus, the neuronal cell death occurred prominently in the CA3 region in contrast to the relatively well-preserved CA1 and CA2 areas. This neuropathology has never been seen in *twitcher* mice on the C57BL/6J background. Biochemically, the brain of *twitcher* mice on the mixed background showed much greater accumulation of lactosylceramide. Genetic background must be carefully taken into consideration when phenotype of mutant mice is evaluated, particularly because most targeted mutants are initially on a mixed genetic background and gradually moved to a pure background. These findings also suggest an intriguing possibility of important function of some sphingolipids in the hippocampal neuronal organization and maintenance.

Key words: Krabbe disease; hippocampus; neuronal cell death; sphingolipids; lactosylceramide

Globoid cell leukodystrophy (GLD; Krabbe disease) is one of the two classic genetic leukodystrophies in humans, together with metachromatic leukodystrophy (Wenger et al., 2001). All known cases of human GLD are caused by deficiency of lysosomal galactosylceramidase (GALC; EC 3.2.1.46). The *twitcher* mouse is a genetically and enzymatically authentic mouse model of human GLD (Kobayashi et al., 1980), and has been used widely for investigation of the pathogenesis and therapeutic trials on GLD (Suzuki and Suzuki, 1995). Commercially available *twitcher* mice are maintained on an inbred C57BL/6J genetic background and they have been used most commonly for these studies. C57BL/6J mice are also used commonly as surrogate mothers in the production of targeted mutants; however, available embryonic stem cells are from mice on the 129Sv background (Fujita et al., 1996; Matsuda et al., 2001a). Nearly all experimental mutants generated with the gene targeting technology are thus initially of mixed genetic background of C57BL/6J and 129Sv, which are inevitably used for initial characterization soon after their production. It is common in many laboratories, however, that the phenotype of such mutants seems to shift in time as the mice are back-crossed to a more homogeneous background. Influence of genetic background on the phenotype of Mendelian single-gene disorders is of great potential importance both in theory and in practice, but most information remains anecdotal and poorly controlled. Evaluation that is more careful is highly desirable.

Contract grant sponsor: National Organization for Rare Disorders, Inc. (NORD); Contract grant sponsor: Japan Society for the Promotion of Sciences; Contract grant number: 11680741, 1550239, 13670016, 14370247.

*Correspondence to: Junko Matsuda, MD, Department of Pediatrics, University of Tokushima School of Medicine, 3-18-15, Kuramoto-cho, Tokushima 770-8503, Japan. E-mail: junko@clin.med.tokushima-u.ac.jp

Received 31 March 2004; Revised 23 April 2004; Accepted 26 April 2004

Published online 16 June 2004 in Wiley InterScience (www.interscience.wiley.com). DOI: 10.1002/jnr.20190

We generated *twitcher* mice that were on a mixed genetic background for 129SvEv and C57BL/6J strains and compared their clinical, neuropathologic, and biochemical manifestations with standard *twitcher* mice on the C57BL/6J background. We found marked effects of genetic background on neurologic, neuropathologic, and biochemical phenotypes in the *twitcher* mice.

MATERIALS AND METHODS

Animals

Mice heterozygous for the *twitcher* mutation, which had been on the C57BL/6J background (Jackson Laboratories, Bar Harbor, ME), were crossed with wild-type mice on a 129SvEv background. Offspring in the F2 generation were genotyped and heterozygotes for the *twitcher* mutation were intercrossed to generate *twitcher* mice on the C57BL/6J-129SvEv mixed background. We then compared their clinical, biochemical, and pathologic phenotype with those of *twitcher* mice on the C57BL/6J background. The genetic status for the *twitcher* mutation was determined by diagnostic PCR on genomic DNA extracted from clipped tails around 5 days postnatally according to the method of Sakai et al. (1996) with some modification (Tohyama et al., 2000). All animals were kept in a specific pathogen- and odor-free environment, and maintained under a 12-hr light/dark cycle at ambient temperature (24 ± 1°C), with food and water available ad lib. For the paralyzed *twitcher* mice, gelatinous high-caloric foods were put on the floor for easy access. The present study was carried out in accordance with the Guidelines for the Care and Use of Laboratory Animal adopted by the Committee on Animal Research in The University of Tokushima, and also accredited by the Japanese Ministry of Education, Culture, Sports, Science, and Technology. Every effort was taken to minimize the number of animals used and any pain or discomfort in all experiments.

Clinical Evaluation

To follow the course of the disease, all mice were observed closely throughout their lives. The day of tremor or seizure onset was noted. Body weight was recorded once a day as an objective parameter for development and progression of the disease. To determine survival time, some mice were allowed to live as long as they could be maintained humanely according to the acceptable practice of laboratory animal care but without forced feeding or other extraneous interventions. More than 10 mice from each group were sacrificed at 30 days for pathologic and biochemical evaluation. For biochemical analyses, samples were stored at −80°C until analyses.

Neuropathology

Tissue preparation. Mice were anesthetized with ether and perfused through the left cardiac ventricle with physiological saline (0.9% NaCl), followed by 4% paraformaldehyde in 0.1 M sodium phosphate buffer (pH 7.4) and immersed in the same fixative at 4°C overnight. The brain, spinal cord, trigeminal, and sciatic nerves were dissected and processed for paraffin sections and immunohistochemical study.

Histopathology and immunohistochemistry. The paraffin sections of the central nervous system (CNS) and peripheral nervous system (PNS) tissues were stained with hematoxylin and eosin and with Luxol fast blue/periodic acid Schiff (LFB-PAS).

For free-floating immunohistochemical studies, the brain was sliced in coronal and parasagittal direction at 50 μm thickness with a microslicer (DTK-1000; Dosaka, Japan). Sections were pretreated by 3% H_2O_2 in 80% methanol for few hours to reduce the endogenous peroxidase activities and to increase the penetration of antibodies. Sections were incubated in the primary antibodies for 1–3 days at 20°C, then in secondary antibodies for 2 hr. The Avidin-biotin complex (ABC) method was then carried out according to the manufacturer's protocol (Vector Labs, Burlingame, CA). Finally, the reaction products were visualized by 0.05% diaminobenzidine tetrahydroxychloride (DAB) containing 0.01% H_2O_2 for 5–10 min at room temperature. After immunostaining, sections were postfixed in 0.05% osmium tetroxide in 0.1 M phosphate buffer for 20 min and dehydrated in a graded series of ethanol, infiltrated in propylene oxide, and flat-embedded in epoxy resin between cover slips and glass slides. Primary antibodies used for the study were as follows: mouse anti-macrophage 1 (Mac1) (Chemicon, Temecula, CA), mouse anti-glial fibrillary acidic protein (GFAP) (Sigma, St. Louis, MO), mouse anti-parvalbumin (PV), (SWant, Switzerland), mouse anti-polysialic acid-neuronal cell adhesion molecule (PSA-NCAM; a gift from Dr. T. Seki, clone number 12E3) (Seki and Arai, 1993), rabbit anti-glutamatic acid decarboxylase (GAD65/67) (Sigma). All primary antibodies were used at 1:5,000 dilution. The secondary antibodies used for the study were as follows: biotinylated horse anti-mouse immunoglobulin (Ig)G for Mac1, GFAP, and PV, biotinylated goat anti-mouse IgM for PSA-NCAM, biotinylated goat anti-rabbit IgG for GAD65/67 (Vector Laboratory). All secondary antibodies were used at 1:200 dilution. Double immunostaining with GAD65/67 and PV was carried out using fluorescent secondary antibodies. After rinsing in PBS, immunostained sections were mounted in Vectashield (Vector) and examined with a confocal laser scanning-light microscopy (TCS-NT; Leica) using laser beams of 488, 568, and 647nm for excitation with appropriate filter sets. Neuronal profiles of PV immunoreactive cells in the hippocampal CA3 region were drawn using a composite camera lucida. The present immunohistochemical methods generally followed our previous study (Toida et al., 1996, 2000).

Timm staining. To visualize the hippocampal mossy fiber terminals, the Neo-Timm method was selected based on the enriched Zn^{2+} in the mossy fiber terminals (Sakata-Haga et al., 2003). Mice were perfused with saline followed by 3% glutaraldehyde containing 0.1% sodium sulfide in 0.1 M phosphate buffer (pH 7.3). Brains were removed and immersed in the same fixative at 4°C. Parasagittal 30-μm thick microslicer sections of the dorsal hippocampus were prepared and mounted on glass slides. Sections were incubated with physical developer (13.2% gum arabic, 1.7% citric acid, 0.57% hydroquinone, and 0.073% silver lactate in distilled water) for 1 hr at 26°C, and then fixed with 5% sodium thiosulfate for 30 min. Some sections were counterstained with cresyl violet (Nissl staining) for observation of structural abnormalities.

Detection of apoptotic cells. Apoptotic cells in the brains of *twitcher* mice were investigated in both genetic back-

grounds by the terminal deoxynucleotidyl nick-end labeling (TUNEL) method. The ApoTag Plus Peroxidase In situ Apoptosis Detection kit for immunoperoxidase staining was used (Intergen, Purchase, NY) according to the manufacturer's protocol with some modifications. Briefly, paraffin-embedded tissue was deparaffinized using xylene and absolute ethanol and then treated with proteinase K. Endogenous peroxidase was then blocked with 2% hydrogen peroxidase solution in methanol (10 min, 43°C). The TUNEL assay was carried out using TdT enzyme followed by treatment with antidigoxigenin peroxidase conjugate. Counterstaining was carried out with methyl green. Additionally, immunostaining with the PV antibody labeled with Vector Red Alkaline Phosphatase Substrate Kit 1 (Vector) was employed to determine the cell phenotype of TUNEL-positive cells.

Lipid Analyses

Lipid extraction from tissues. Tissues (brain, liver and kidney) were homogenized with water at 20% of concentration by weight in an all-glass Potter-Elvehjem homogenizer. Initial extraction with chloroform-methanol was carried out as described previously (Fujita et al., 1996). Lipids were fractionated to neutral and acidic fractions using the reverse-phase column essentially using Kyrklund's method (Kyrklund, 1987) (Bond Elute C-18, 3 ml/500 mg; Varian, Inc., Palo Alto, CA). Aliquots of the brain neutral lipid fraction were subjected to the mercuric chloride-saponification procedure to remove essentially all glycerophospholipids (Abramson et al., 1965).

Thin-layer chromatography and quantitation of lactosylceramide. Thin-layer chromatography (TLC) and quantitation of tissue lipids, except for psychosine, were done with Merck high-performance TLC plates (Silica gel 60; Merck, Germany), with appropriate solvents and sprays for separation and visualization and quantitation as previously described (Fujita et al., 1996).

Quantitation of psychosine. Brain psychosine (galactosylsphingosine) was determined by the high-performance liquid chromatography (HPLC) procedure as modified recently by us (Matsumoto et al., 1997). The brain homogenates containing approximately 3 mg protein were added to 3 ml of chloroform-methanol (1:2 vol/vol) containing 400 pmol of eicosasphinganine as an internal standard, thoroughly mixed with a vortex stirrer for 30 sec and kept for 30 min at room temperature with occasional additional shaking. The extracted lipid fraction was freed of insoluble material by centrifugation and decanting to another tube and evaporated to dryness under a flow of nitrogen at 37°C. It was redissolved in 0.9 ml of chloroform-methanol (1:2 vol/vol) and glycolipids were saponified with addition of 0.1 ml of 1 N NaOH for 2 hr at 37°C with occasional shaking. At the end of the saponification procedure, 0.1 ml of chloroform-methanol (1:2 vol/vol), 1 ml of chloroform, and 0.4 ml of water were added and the solutes were partitioned into the aqueous phase and organic phase. The upper aqueous phase was removed and the lower phase was washed twice with addition of 1 ml of alkaline theoretical upper phase (chloroform:methanol: 0.8 mM ammonia water, 3:48:47 by volume). After evaporation of the organic phase at 37°C under a flow of nitrogen, long-chain bases redissolved in 50 μl of methanol were derivatized at room temperature for 15 min by addition of 50 μL of the *o*-phthalaldehyde reagent. The reaction was stopped by addition of the mobile phase (14:1 vol/vol methanol:5 mM sodium phosphate buffer, pH 7.0) with 50 mg/l sodium octylsulfate as an ion-pairing agent. The HPLC analysis was carried out using a Shimadzu LC-6A pump with a column (CAPCELL PAK C18 UG120, S-5 μm, 250 × 4.6 mm, SHISEIDO, Japan) and detection with a Fluorescent Detector (HITACHI, L-7480) (excitation wavelength 340 nm, emission wavelength 455 nm). The solvent system was 14:1 methanol:5 mM sodium phosphate buffer, pH 7.0 (vol/vol), with 50 mg/l sodium octylsulfate. The flow rate was 0.6 ml/min. An integrated Shimadzu data system C-R4A CHROMATOPAC controlled the chromatography unit including the autosampler (Shimadzu, SIL-6B, and SCL-6B) and provided computerized data analysis. The peaks of psychosine (galactosylsphingosine), sphingosine, sphinganine, and eicosasphinganine (internal standard) were eluted in this order and were separated cleanly from each other and from other interfering fluorescent materials. The tissue levels of psychosine corrected for the internal standard and the relative detector response were expressed in pmol/mg tissue protein. The data were evaluated by unpaired Student's *t*-test.

Enzymic Assay

Assay for acid β-galactosidase was carried out on brains of 30-day-old mice of each genotype as described previously (Tohyama et al., 2000). Brains were homogenized with double-distilled water (20% wt/vol). The protein content was determined using a Bio-Rad DC protein assay kit (Bio-Rad, Hercules, CA). Activity of acid β-galactosidase was determined with 4-methylumbelliferyl-β-galactoside (Sigma).

RESULTS

Clinical Phenotype

Twitcher mice on the C57BL/6J-129SvEv mixed background showed clinical phenotype such as stunted growth, twitching, and hindleg weakness similar to *twitcher* mice on the C57BL/6J background. The *twitcher* mice on the C57BL/6J-129SvEv mixed background, however, were smaller than were *twitcher* mice on the C57BL/6 background (body weight at 30 days = 7.6 ± 1.0 g, n = 9, vs. 10.5 ± 1.3 g, n = 3; P = 0.003). Most markedly, many *twitcher* mice on the C57BL/6J-129SvEv mixed background showed frequent epileptic seizures around 25 days of age. These neurologic symptoms have practically never been seen in the *twitcher* mice on the C57BL/6 background. Their average lifespan was shorter (33 ± 6 days, n = 11) than was that of *twitcher* mice on the C57BL/6 background (48 ± 5 days, n = 41).

Neuropathologic Phenotype

In both genetic backgrounds, severe demyelination with infiltration of macrophages containing PAS-positive materials were seen in both the CNS and PNS at 30 days. The degree of demyelination of *twitcher* mice on the C57BL/6J-129SvEv mixed background was as severe as that of *twitcher* mice on the C57BL/6J background both in the CNS and PNS (Fig. 1). At 30 days, however, the standard histologic evaluation of *twitcher* mice on the

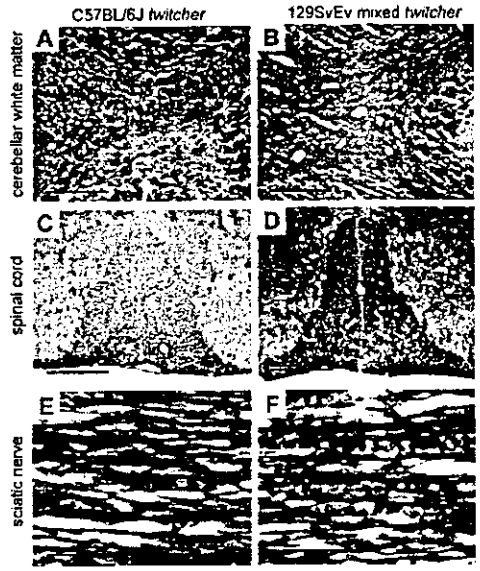

Fig. 1. Comparison of the degree of demyelination in *twitcher* mice on both strains at 30 days. Luxol-fast blue (LFB)-periodic acid Schiff (PAS) stain. In both strains, the degree of demyelination with infiltration of PAS-positive macrophages was similar in both CNS and PNS. Arrow, PAS-positive macrophages; arrowhead, myelin droplet. **A, C, E:** *Twitcher* mice on the C57BL/6 background. **B, D, F:** *Twitcher* mice on the C57BL/6J-129SvEv mixed background. Upper column, CNS cerebellar white matter; middle column, spinal cord (anterior column); lower column, PNS sciatic nerve. Scale bars = 200 μm (A–D); 100 μm (E, F).

C57BL/6J-129SvEv mixed background revealed apparent neuronal cell death in the cortex and hippocampus of the brain, most prominently in the CA3 region of the hippocampus (Fig. 2). In the hippocampus, the neuronal cell death occurred prominently in the CA3 region in contrast to the relatively well-preserved CA1 and CA 2 areas. Neuronal cell death was observed as early as 20 days and progressed rapidly toward the terminal stage. In the terminal stage, around 35–40 days, almost all hippocampal CA3 pyramidal neurons were depleted and replaced by astrocytic gliosis. Some cells in the hippocampal CA3 area were TUNEL positive and certain numbers of the TUNEL-labeled cells revealed nuclear morphologic features of apoptosis (Fig. 3). These neuropathologic changes in neurons have never been observed in *twitcher* mice on the inbred C57BL/6J background, even at their terminal stage of around 45 days. In addition, no pathologic changes have been observed in the brain of heterozygotes for the *twitcher* mutation, not only in the 129SvEv strain but also in the C57BL/6J strain. To investigate further the changes in the hippocampal formation in *twitcher* mice on the C57BL/6J-129SvEv mixed background, we carried out immunohistochemical studies using several antibodies of glial and neuronal cell markers. Increased immunoreactivity of Mac1 and GFAP, which are markers for microglia/macrophage and astroglial cells, respectively, was observed around the CA3 area of the hippocampus, suggesting the early and marked activation of microglial and astroglial cells in this area (Fig. 4). Immunoreactivity of PSA-NCAM, which is a marker for newly generated neurons, was strongly positive in the mossy fibers of the hippocampal formation of wild-type mice or *twitcher* mice on the C57BL/6J background. In contrast, it was decreased progressively to the terminal stage of *twitcher* mice on the C57BL/6J-129SvEv mixed background. Timm staining also showed irregular and abnormal synapse formation in the hippocampal CA3 area in *twitcher* mice on the C57BL/6J-129SvEv mixed background (Fig. 5). The immunostaining of parvalbumin (PV), which is a marker for the inhibitory GABAergic interneuron, showed markedly suppressed dendrite extension only in *twitcher* mice on the C57BL/6J-129SvEv mixed background (Fig. 6). Furthermore, the double immunostaining study with PV and GAD65/67, both markers for GABAergic interneurons, showed abnormal GAD-immunoreactivity of the PV somata, and detachment of axosomatic contacts (possibly suppression of GABAergic synaptic contacts to PV somata) in *twitcher* mice on the C57BL/6J-129SvEv mixed background (Fig. 7). A double-staining study for PV and TUNEL showed that PV-positive interneurons in the CA3 area were not TUNEL positive (data not shown), although they showed poor dendrite extension and abnormal synaptogenesis.

Biochemical Phenotype

Sphingolipids from the brain, liver, and kidney were examined by TLC at 30 days. The lipid profiles were similar generally, except that there was a significant additional accumulation of lactosylceramide only in the brain of *twitcher* mice on the C57BL/6J-129SvEv mixed background. Its level in the brain of the C57BL/6J-129SvEv *twitcher* mice was more than 10 times that of the level in the C57BL/6J *twitcher* mice (Fig. 8). In contrast, in the liver and kidney, we did not observe significant differences in lactosylceramide accumulation in *twitcher* mice of both genetic backgrounds.

Psychosine (galactosylsphingosine) is highly cytotoxic and is a substrate of GALC. Experimental evidence has been accumulating in support of a hypothesis that psychosine accumulation may be responsible primarily for the disappearance of myelinating cells in GLD (Miyatake and Suzuki, 1972; Igisu and Suzuki, 1984; Suzuki, 1998).

Psychosine accumulates 10–20-fold in human patients with GLD as well as in GLD that occurs in other mammalian species, including *twitcher* mice. Psychosine levels in the brain from 30-day-old *twitcher* and wild-type mice on each genetic background were analyzed by the HPLC procedure. Despite the marked difference in neurologic and neuropathologic severity, the brain psychosine levels of 129SvEv xC57BL/6J *twitcher* mice were similar to that of C57BL/6J *twitcher* mice ($P = 0.39$) (in pmol psychosine/mg protein, mean ± SD of C57BL/6J wild-type: 16.8 ± 2.6, $n = 5$; 129SvEv xC57BL/6J wild-type

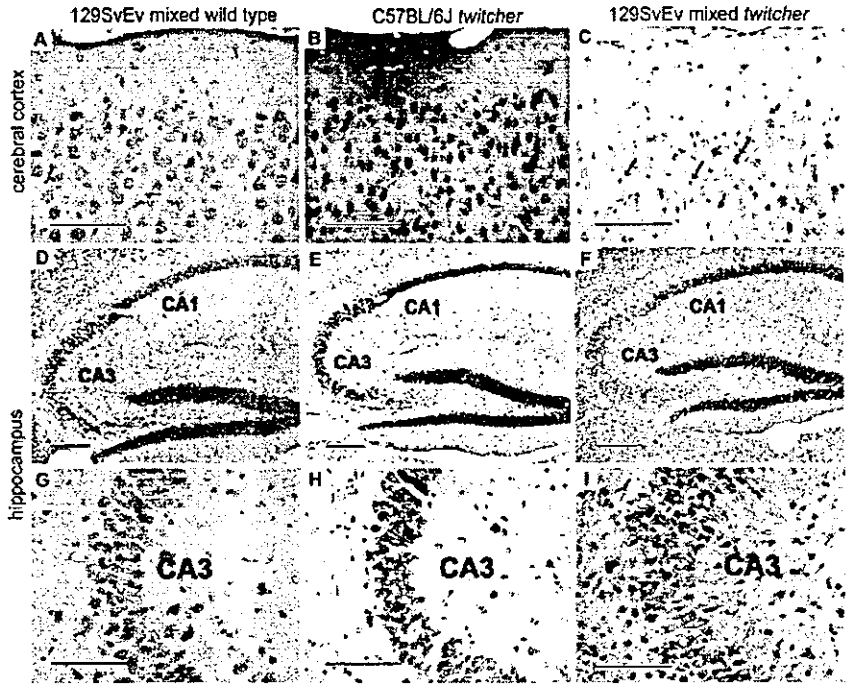

Fig. 2. Neuropathology of *twitcher* mice on both strains at 30 days. Compared to the wild-type (**A, D, G**) and *twitcher* mice on the C57BL/6J background (**B, E, H**), only in *twitcher* mice on the C57BL/6J-129SvEv mixed background was apparent neuronal cell death in the cortex and hippocampus CA3 area observed (**C, F, I**). In the hippocampus, the neuronal cell death occurred prominently in the CA3 region in contrast to the well-preserved CA1 and CA 2 areas. Many degenerating neurons with pyknotic nuclei and eosinophilic cytoplasm were evident (arrow). CA1 and CA2 regions contained much fewer degenerating neurons. Upper column, cerebral cortex; middle column, hippocampus; lower column, hippocampus CA3 area. All were HE stained. Scale bars = 100 μm (A–C, G–I); 200 μm (D–F).

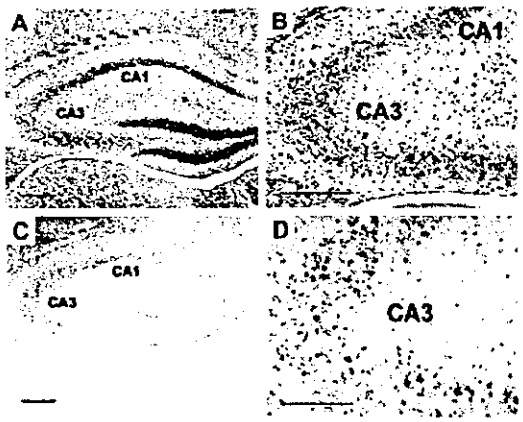

Fig. 3. Neuronal cell death in the hippocampal CA3 area of *twitcher* mice on the C57BL/6J-129SvEv mixed background. Certain numbers of cells in the hippocampal CA3 area were TUNEL positive, suggesting the apoptotic cell death in these areas. HE (**A, B**) and TUNEL stained (**C, D**). Scale bars = 200 μm (A,C); 100 μm (B, D).

mice;15.4 ± 3.8, $n = 5$; C57BL/6J *twitcher* mice: 119.0 ± 9.1, $n = 5$; 129SvEv xC57BL/6J *twitcher* mice: 125.1 ± 12.6, $n = 6$).

Because there was an increase in lactosylceramide in the brain of *twitcher* mice on the C57BL/6J-129SvEv mixed background, acid β-galactosidase activity in the brain from 30-day *twitcher* and wild-type mice on each genetic background was analyzed. There was no significant difference in the acid β-galactosidase activity between the two strains, in either wild-type mice ($P = 0.29$) or in the *twitcher* mice ($P = 0.27$) (in nmol /hr/mg protein, mean ± SD for C57BL/6J wild-type: 69.5 ± 10.2, $n = 5$; 129SvEv xC57BL/6J wild-type mice: 63.4 ± 6.7, $n = 5$; C57BL/6J *twitcher* mice: 68.4 ± 8.8, $n = 5$; 129SvEv xC57BL/6J *twitcher* mice: 59.9 ± 13.8, $n = 6$).

DISCUSSION

The series of observations described in this report clearly indicate that the genetic background contributes significantly to the phenotype of the *twitcher* mutant caused by a mutation in the GALC gene. There have been earlier sporadic reports that suggested a similar conclusion. For example, Duchen et al. (1980), in their original description of the *twitcher* mutant, noted that *twitcher* mice on the

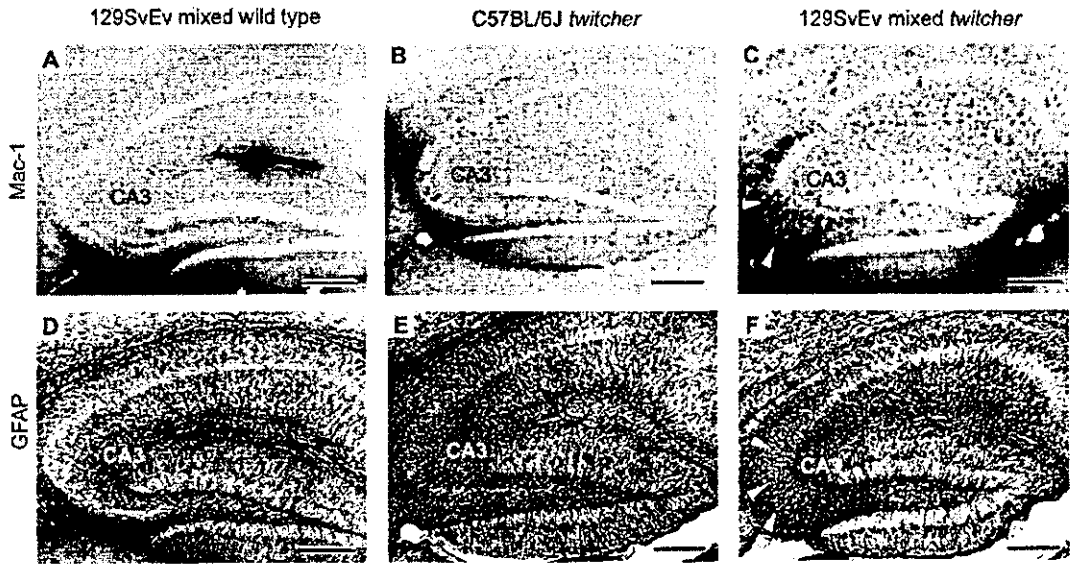

Fig. 4. Immunohistochemical findings for Mac1 and GFAP in the hippocampus of *twitcher* mice on both strains. Upper column, anti Mac1 antibody; lower column, anti-GFAP antibody. Compared to wild type (**A, D**), increased immunoreactivity of Mac1 and GFAP, which are markers for microglia/macrophage and astroglial cells, respectively, was observed in *twitcher* mice on both strains (**B, C, E, F**). In *twitcher* mice, however, on the C57BL/6J-129SvEv mixed background, remarkably increased immunoreactivity around the CA3 area of the hippocampus was observed, reflecting the marked activation of microglial cells and astroglial cells in these areas (C, F; arrowheads). Scale bars = 200 μm.

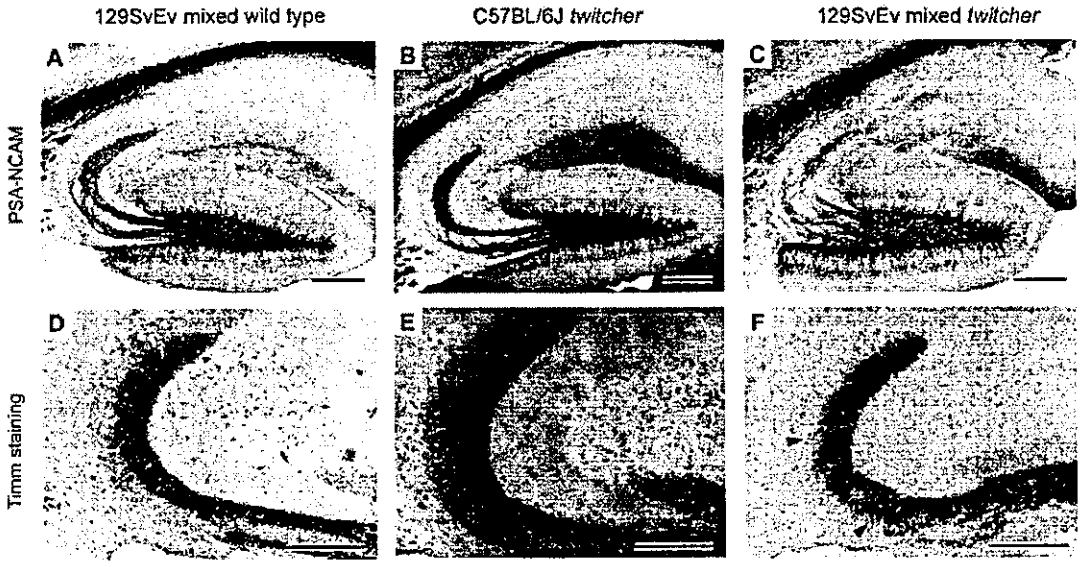

Fig. 5. Immunostaining for PSA-NCAM and Timm staining in the hippocampus of *twitcher* mice on both strains. Immunoreactivity of PSA-NCAM was highly positive in mossy fibers of the hippocampal formation in wild-type or *twitcher* mice on the C57BL/6J background (**A, B**), and was decreased in *twitcher* mice on the C57BL/6J-129SvEv mixed background (**C**). Timm staining (lower column) showed the irregular and abnormal synapse formation at the hippocampal CA3 area in *twitcher* mice on the C57BL/6J-129SvEv mixed background (**D–F**). E had greater counter-staining by cresyl violet, but not in the Timm staining itself. Scale bars = 200 μm.

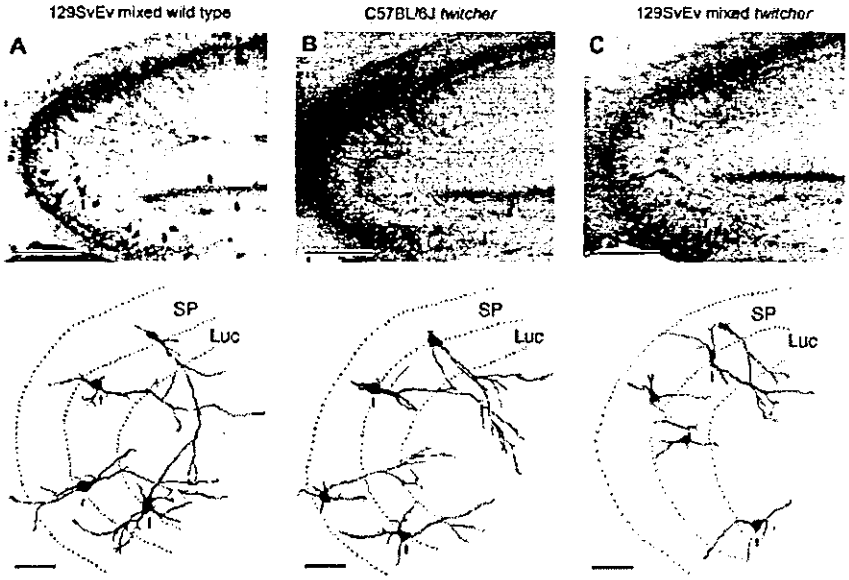

Fig. 6. Immunohistochemical findings for PV in the hippocampus of *twitcher* mice on both strains. Compared to the marked extension of the dendrite of the PV-positive neurons in the hippocampal CA3 area in wild-type and *twitcher* mice on the C57BL/6J background (**A, B**), the dendrite extension of the *twitcher* mice on the C57BL/6J-129SvEv mixed background was clearly suppressed (**C**). Lower column shows the manually drawn neuronal profiles of PV immunoreactive cells in the hippocampal CA3 region. Arrow, same neuron in each upper column. Scale bars = 200 μm (upper column); 50 μm (lower column). SP, stratum pyramidale; Luc, lucidum.

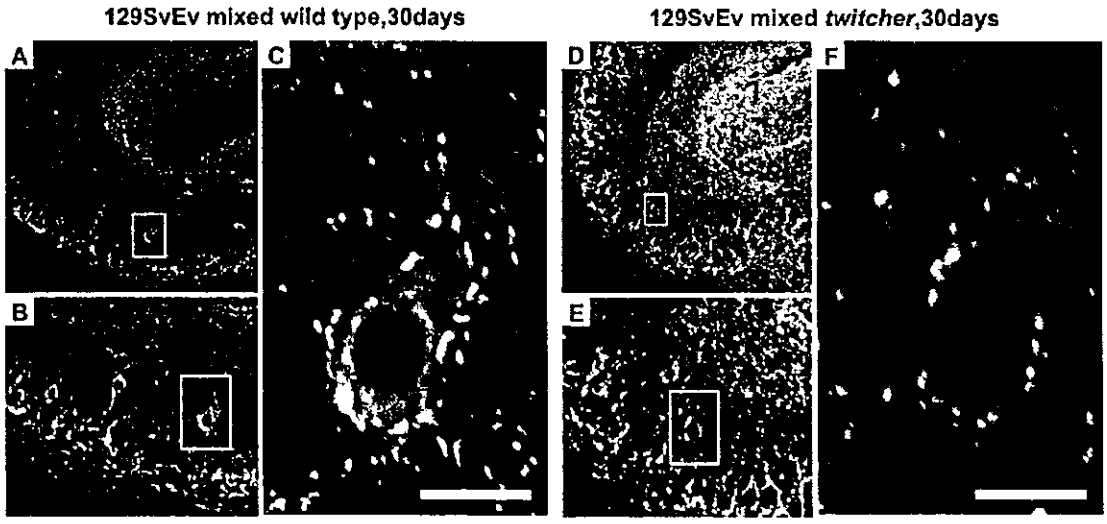

Fig. 7. Double immunostaining with PV and GAD65/67 in the hippocampus of *twitcher* mice on both strains. Compared to the well-organized synapse formation between inhibitory GABAergic interneurons in wild type (**C**), abnormality of the cell body structure, suppressed dendrite extension, and decreased synapse formation were observed in *twitcher* mice on the C57BL/6J-129SvEv mixed background (**F**). White squares indicate the neuron shown in the higher magnification images. Scale bars = 10 μm.

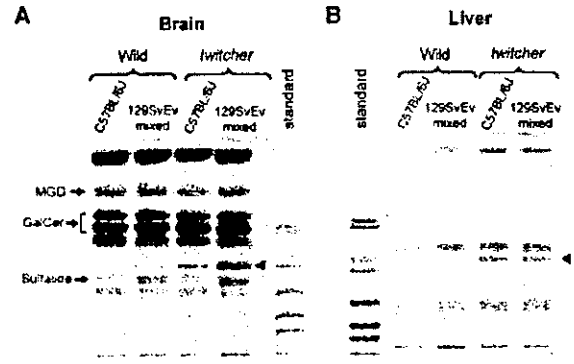

Fig. 8. Thin-layer chromatography of lipids from the brain and liver of *twitcher* mice on both strains. Solvent system was chloroform:methanol: water (65:25:4 by volume). Detection was carried out by orcinol spray. A 5-mg wet weight-equivalent sample from the brain and 10-mg wet weight-equivalent sample from liver were applied on the plate (arrowhead, lactosylceramide). Compared to the wild-type and *twitcher* mice on the C57BL/6J background, *twitcher* mice on the C57BL/6J-129SvEv mixed background showed massive accumulation of lactosylceramide in the brain (**A**). In contrast, in the liver, no apparent difference in the degree of accumulation of lactosylceramide was detected between *twitcher* mice on these two strains (**B**).

CE/J × C57BL/6J mixed background had a milder course than did *twitcher* mice on the C57BL/6J background. More recently, Biswas et al. (2002) described delayed clinical and pathologic signs in *twitcher* mice on the C57BL/6 × CAST/Ei background. We found *twitcher* mice on the C57BL/6J-129SvEv mixed background had a more severe disease with a shorter lifespan, generalized seizures, massive neuronal cell death, most prominently in the CA3 area of hippocampus, and a significant accumulation of lactosylceramide in the brain. These neurologic manifestations never occur in *twitcher* mice on the inbred C57BL/6 background, except when *twitcher* mice are also simultaneously heterozygous for a mutation in the other lysosomal β-galactosidase, GM1-ganglioside β-galactosidase (Tohyama et al., 2000).

The selective and almost complete neuronal loss in the CA3 region of the hippocampus, observed in *twitcher* mice on the C57BL/6J-129SvEv mixed background, is unusual. Neuronal loss in the hippocampal CA3 region was much greater than that in the other areas of the brain, including the CA1 and CA2 regions of the hippocampus, dentate gyrus, and cortex. Glutamate excitotoxicity plays a key role in inducing neuronal cell death in many neurologic diseases. In mice, administration of kainic acid, an analogue of the excitotoxin glutamate, results in seizures and neuronal cell death most prominently in the CA3 area and in the CA1 area (Pollard et al., 1994; Kurschner et al., 1998). Global ischemia in the mouse elicits damage confined almost exclusively to CA1 neurons of the hippocampus (Penahian et al., 1996; Sheng et al., 1999). The pattern of hippocampal neuronal death that was observed in *twitcher* mice on the C57BL/6J-129SvEv mixed background was different from that seen in other experimental conditions of brain injury.

Strain differences in the vulnerability of the hippocampus are also known (Schauwecker and Steward, 1997; Shuttleworth and Connor, 2001). The largest known differences in hippocampal neurogenesis are between C57BL/6 and 129SvJ mice, which are the two strains that are used widely to generate transgenic or knockout animals (Kempermann et al., 1997). The 129SvJ mice have the lowest number of surviving newborn cells and are seizure or excitotoxicity sensitive compared to the resistant C57BL/6 strain. Little is known about the distinct factors that cause the strain differences of the hippocampal vulnerability. Our results seem consistent with this known difference between the two strains of mice in terms of vulnerability of hippocampal neurons to endogenous or exogenous insults.

To gain insight into the mechanism of neuronal death in the hippocampus, a series of immunohistochemical studies were carried out using various glial and neuronal cell markers (Mac1, GFAP, PV, GAD65/67, and PSA-NCAM). We found changes in several glial and neuronal cell markers in the CA3 area. The increased immunoreactivity of the Mac1 and GFAP in the hippocampal CA3 area may represent immediate reactions to the beginning of cell death in the CA3 pyramidal neurons. The activated glial cells could exacerbate cell death and initiate a vicious cycle. The suppressed dendritic extension or synaptic formation of PV-positive neurons in the hippocampus may cause hyperexcitability through depletion of inhibitory inputs from the GABAergic inhibitory neurons. PSA-NCAM, a marker for newly developing neurons, was strongly positive in mossy fibers of the normal hippocampal formation. In mammals, neuronal stem cells or progenitor cells are present in two regions: the subventricular zone of the forebrain and the subgranular zone of the dentate gyrus (Gould et al., 1999). Hippocampal mossy fibers are axons projecting from dentate granule cells to the apical dendrites of CA3 pyramidal cells. Mossy fiber extension and maintenance are supposed to be for normal hippocampal function, including memory. In temporal lobe epilepsy of human or experimental animals, mossy fiber innervation was noted (McNamara, 1994). The suppressed PSA-NCAM immunoreactivity and abnormal synaptogenesis in the mossy fiber, observed in *twitcher* mice on the C57BL/6J-129SvEv mixed background, may contribute at least in part to excitability, seizures, and CA3 pyramidal neuronal death. We also have to rule out the possibility that neuronal cell death in the hippocampus is a secondary change due to epileptic seizures (McNamara, 1994).

Biochemical pathogenesis of the observed neurologic and neuropathologic abnormalities should also be considered. Ever since it was proposed in 1972, the aberrant metabolite of galactosylceramide, psychosine (galactosylsphingosine), has been well established as the cytotoxic compound responsible for much of GLD

pathogenesis (Miyatake and Suzuki, 1972; Suzuki, 1998). Our analytical data, however, clearly indicate that psychosine is not responsible for these additional neurologic manifestations. This is not surprising, because the same galactosyltransferase synthesizes both galactosylceramide and psychosine and no other metabolic pathways are known to generate psychosine (Coetzee et al., 1996). Because of its nearly exclusive localization in the myelin sheath, this synthetic pathway also occurs exclusively in actively myelinating cells; therefore psychosine is a priori unlikely to be the cause of the neuronal pathology.

More intriguing is the much higher accumulation of lactosylceramide in the brain only in *twitcher* mice on the mixed background. In human and mouse, the two lysosomal β-galactosidases, galactosylceramidase (GALC) and acid β-galactosidase (BGAL), share substrate specificity to degrade lactosylceramide (Tanaka and Suzuki, 1976). It is known that tissue activities of acid β-galactosidase vary in different strains of mice (Felton et al., 1974; Bouvier and Seyfried, 1990). This factor might be responsible for lactosylceramide accumulation in the brain of *twitcher* mice on the mixed background. Because the *twitcher* mutation abolishes almost completely the galactosylceramidase activity, we have measured acid β-galactosidase activity in the brain from *twitcher* and wild-type mice on both strains of C57BL/6 and 129SvEv to see whether there are any differences in acid β-galactosidase activity. We found no significant difference in the acid β-galactosidase activity between these two strains, however, not only in wild-type mice but also in the *twitcher* mice. Lactosylceramide accumulation in the *twitcher* mice of mixed genetic background therefore cannot be explained based on possible strain difference in acid β-galactosidase activity.

The nervous system is rich in sphingolipids, and their physiologic functions are drawing closer attention because of their newly found functions in a variety of cellular processes including differentiation, apoptosis, and proliferation (Hakomori, 2000; Lusa et al., 2001; Gulbins and Kolesnick, 2003; Hering et al., 2003). Several signal molecules are localized in a glycolipid-enriched microdomain on the cell surface, and their signals are regulated by glycolipid composition. The microdomains form functional units, termed lipid rafts or caveolae, which mediate signal transduction and cell functions (Hakomori, 2000). Recent studies on lactosylceramide have suggested its functional significance in human neutrophil and epithelial cells (Iwamoto et al., 2001; Iwabuchi and Nagaoka, 2002). Lactosylceramide-enriched microdomains activate NADPH and initiate a signal transduction pathway leading to superoxide generation. It is therefore tempting to hypothesize that the lactosylceramide accumulation in the *twitcher* mice on the C57BL/6J-129SvEv mixed background might be related causally to their neurologic abnormalities.

Our observations also have clinical implications. The clinical manifestations of human GLD are classified into the most typical infantile form, and more infrequent late infantile, juvenile, and adult forms (Kolodny et al., 1991; Wenger et al., 2001). In human GLD patients, variable clinical courses are observed even in the same family, suggesting some modifying factors (Wenger et al., 2001). Some of these factors may be epigenetic, such as the marked effect of pregnancy on the course of the recently generated mouse model of late-onset, chronic form of GLD (Matsuda et al., 2001b) but some others may well be genetic. This genetic makeup of humans is exceedingly complex, and dissecting out these factors will require extensive future studies.

Although the precise molecular mechanisms remain unclear, our in vivo findings in this study suggest the possible important role of sphingolipids in the nervous system, particularly in hippocampal neuronal organization. Furthermore, understanding of the molecular mechanisms underlying hippocampal CA3 neuronal cell death may help in the design of novel neuroprotective strategies for intervention in the neuronal death associated with sphingolipidosis or other neurologic disorders, including epilepsy and Alzheimer's disease.

ACKNOWLEDGMENTS

This work was supported by the National Organization for Rare Disorders, Inc. (NORD) (Roscoe Brady Lysosomal Storage Diseases Fellowship to J.M.) and by Grant-in-aids for Scientific Research from the Japan Society for the Promotion of Sciences (grant 11680741 and 1550239 to K.T., 13670016 to K.I., and 14370247 to Y.K.).We thank Dr. T. Seki for his kind gift of the PSA-NCAM antibody. We also thank Drs. M.T. Vanier and K. Ohno for helpful comments in psychosine analysis.

REFERENCES

Abramson MB, Norton WT, Katzman R. 1965. Study of ionic structure in phospholipids by infrared spectra. J Biol Chem 240:2389–2395.

Biswas S, Biesiada H, Williams TD, LeVine SM. 2002. Delayed clinical and pathological signs in twitcher (globoid cell leukodystrophy) mice on a C57BL/6 × CAST/Ei background. Neurobiol Dis 10:344–357.

Bouvier JD, Seyfried TN. 1990. Ganglioside GM1 elevation in DBA/2 mouse embryos Dev Neurosci 12:126–132.

Coetzee T, Fujita N, Dupree J, Shi R, Blight A, Suzuki K, Suzuki K, Popko B. 1996. Myelination in the absence of galactocerebroside and sulfatide: normal structure with abnormal function and regional instability. Cell 86:209–219.

Duchen LW, Eicher EM, Jacobs JM, Scaravilli F, Teixeira F. 1980. Hereditary leukodystrophy in the mouse: the new mutant twitcher. Brain 103:695–710.

Felton J, Meisler M, Paigen K. 1974. A locus determining beta-galactosidase activity in the mouse. J Biol Chem 249:3267–3272.

Fujita N, Suzuki K, Vanier MT, Popko B, Maeda N, Klein A, Henseler M, Sandhoff K, Nakayasu H, Suzuki K. 1996. Targeted disruption of the mouse sphingolipid activator protein gene: a complex phenotype, including severe leukodystrophy and wide-spread storage of multiple sphingolipids. Hum Mol Genet 5:711–725.

Gould E, Beylin A, Tanapat P, Reeves A, Shors TJ. 1999. Learning enhances adult neurogenesis in the hippocampal formation. Nat Neurosci 2:260–265.

Gulbins E, Kolesnick R. 2003. Raft ceramide in molecular medicine. Oncogene 22:7070–7077.

Hakomori SI. 2000. Cell adhesion/recognition and signal transduction through glycosphingolipid microdomain. Glycoconj J 17:143–151.

Hering H, Lin CC, Sheng M. 2003. Lipid rafts in the maintenance of synapses, dendritic spines, and surface AMPA receptor stability. J Neurosci 23:3262–3271.

Igisu H, Suzuki K. 1984. Progressive accumulation of toxic metabolite in a genetic leukodystrophy. Science 224:753–755.

Iwabuchi K, Nagaoka I. 2002. Lactosylceramide-enriched glycosphingolipid signaling domain mediates superoxide generation from human neutrophils. Blood 100:1454–1464.

Iwamoto T, Fukumoto S, Kanaoka K, Sakai E, Shibata M, Fukumoto E, Inokuchi Ji J, Takamiya K, Furukawa K, Furukawa K, Kato Y, Mizuno A. 2001. Lactosylceramide is essential for the osteoclastogenesis mediated by macrophage-colony-stimulating factor and receptor activator of nuclear factor-kappa B ligand. J Biol Chem 276:46031–4608.

Kempermann G, Kuhn HG, Gage FH. 1997. Genetic influence on neurogenesis in the dentate gyrus of adult mice. Proc Natl Acad Sci USA 94:10409–10414.

Kobayashi T, Yamanaka T, Jacobs JM, Teixeira F, Suzuki K. 1980. The twitcher mouse: an enzymatically authentic model of human globoid cell leukodystrophy (Krabbe disease). Brain Res 202:479–483.

Kolodny EH, Raghavan S, Krivit W. 1991. Late-onset Krabbe disease (globoid cell leukodystrophy): clinical and biochemical features of 15 cases. Dev Neurosci 13:232–239.

Kurschner VC, Petruzzi RL, Golden GT, Berrettini WH, Ferraro TN. 1998. Kainate and AMPA receptor binding in seizure-prone and seizure-resistant inbred mouse strains. Brain Res 780:1–8.

Kyrklund T. 1987. Two procedures to remove polar contaminants from a crude brain lipid extract by using prepacked reverse-phase columns. Lipids 22:274–277.

Lusa S, Blom TS, Eskelinen EL, Kuismanen E, Mansson JE, Simons K, Ikonen E. 2001. Depletion of rafts in late endocytic membranes is controlled by NPC1-dependent recycling of cholesterol to the plasma membrane. J Cell Sci 114:1893–1900.

Matsuda J, Vanier MT, Saito Y, Tohyama J, Suzuki K, Suzuki K. 2001a. A mutation in the saposin A domain of the sphingolipid activator protein (prosaposin) gene causes a late-onset, slowly progressive form of globoid cell leukodystrophy in the mouse. Hum Mol Genet 10:1191–1199.

Matsuda J, Vanier MT, Saito Y, Suzuki K, Suzuki K. 2001b. Dramatic phenotypic improvement during pregnancy in a genetic leukodystrophy: estrogen appears to be a critical factor. Hum Mol Genet 10:2709–2715.

Matsumoto A, Vanier MT, Oya Y, Kelly D, Popko B, Wenger DA, Suzuki K, Suzuki K. 1997. Minimal increment in galactosylceramidase expression is sufficient for significant phenotypic improvement in twitcher mouse. Dev Brain Dysfunct 10:142–154.

McNamara JO. 1994. Cellular and molecular basis of epilepsy. J Neurosci 14:3413–3425.

Merrill Jr AH, Wang E, Mullins RE, Jamison WC, Nimkar S, Liotta DC. 1988. Quantitation of free sphingosine in liver by high-performance liquid chromatography. Anal Biochem 171:373–381.

Miyatake T, Suzuki K. 1972. Globoid cell leukodystrophy: additional deficiency of psychosine galactosidase. Biochem Biophys Res Commun 48:538–543.

Penahian N, Yoshida T, Huang PL, Hedley-Whyte ET, Dalkara T, Fishman MC, Moskowitz MA. 1996. Attenuated hippocampal damage after global cerebral ischemia in mice mutant in neuronal nitric oxide synthase. Neuroscience 72:343–354.

Pollard H, Charriaut-Marlangue C, Cantagrel S, Represa A, Robain O, Moreau J, Ben-Ari Y. 1994. Kainate-induced apoptotic cell death in hippocampal neurons. Neuroscience 63:7–18.

Sakai N, Inui K, Tatsumi N, Fukushima H, Nishigaki T, Taniike M, Nishimoto J, Tsukamoto H, Yanagihara I, Ozone K, Okada S. 1996. Molecular cloning and expression of cDNA for murine galactocerebrosidase and mutation analysis of the twitcher mouse, a model of Krabbe's disease. J Neurochem 66:1118–1124.

Sakata-Haga H, Sawada K, Ohta K, Cui C, Hisano S, Fukui Y. 2003. Adverse effects of maternal ethanol consumption on development of dorsal hippocampus in rat offspring. Acta Neuropathol (Berl) 105:30–36.

Schauwecker PE, Steward O. 1997. Genetic determinants of susceptibility to excitotoxic cell death: implications for gene targeting approaches. Proc Natl Acad Sci USA 94:4103–4108.

Seki T, Arai Y. 1993. Highly polysialylated neural cell adhesion molecule (NCAM-H) is expressed by newly generated granule cells in the dentate gyrus of the adult rat. J Neurosci 13:2351–2358.

Sheng H, Laskowitz DT, Pearlstein RD, Warner DS. 1999. Characterization of a recovery global cerebral ischemia model in the mouse. J Neurosci Methods 88:103–109.

Shuttleworth CW, Connor JA. 2001. Strain-dependent differences in calcium signaling predict excitotoxicity in murine hippocampal neurons. J Neurosci 21:4225–4236.

Suzuki K. 1998. Twenty five years of the psychosine hypothesis: a personal perspective of its history and present status. Neurochem Res 23:251–259.

Suzuki K, Suzuki K. 1995. The twitcher mouse: a model for Krabbe disease and for experimental therapies. Brain Pathol 5:249–258.

Tanaka H, Suzuki K. 1976. Specificities of the two genetically distinct β-galactosidases in human sphingolipidoses. Arch Biochem Biophys 175: 332–340.

Tohyama J, Vanier MT, Suzuki K, Ezoe T, Matsuda J, Suzuki K. 2000. Paradoxical influence of acid β-galactosidase gene dosage on phenotype of the twitcher mouse (genetic galactosylceramidase deficiency). Hum Mol Genet 9:1699–1707.

Toida K, Kosaka K, Heizmann CW, Kosaka T. 1996. Electron microscopic serial-sectioning/reconstruction study of parvalbumin-containing neurons in the olfactory bulb. Neuroscience 72:449–446.

Toida K, Kosaka K, Aika Y, Kosaka T. 2000. Chemically defined neuron groups and their subpopulations in the glomerular layer of the rat main olfactory bulb: IV. Intraglomerular synapses of tyrosine hydroxylase-immunoreactive neurons. Neuroscience 101:11–17.

Wenger DA, Suzuki K, Suzuki Y, Suzuki K. 2001. Galactosylceramide lipidosis: globoid cell leukodystrophy (Krabbe disease). In: Scriver CR, Beaudet AL, Sly WS, Valle D, Childs B, Vogelstein B, editors. Metabolic and molecular basis of inherited disease. New York: McGraw-Hill. p 3669–3694.

Clinical Endocrinology (2004) 61, 418–423 doi: 10.1111/j.1365-2265.2004.02041.x

Plasma adiponectin levels in newborns are higher than those in adults and positively correlated with birth weight

Yumiko Kotani, Ichiro Yokota, Seiko Kitamura, Junko Matsuda, Etsuo Naito and Yasuhiro Kuroda
Department of Pediatrics, School of Medicine, University of Tokushima, Tokushima, Japan

(Received 30 July 2003; returned for revision 23 September 2003; finally revised 10 February 2004; accepted 16 March 2004)

OBJECTIVE The aim of this study was to examine plasma adiponectin concentrations during perinatal the period and their correlations with fetal anthropometric parameters and other hormones.

DESIGN Venous cord blood samples were obtained from 59 full-term healthy newborns (36 males and 23 females, gestational age 37·0–41·4 weeks, birth weight 2,146–4,326 g, birth length 44·0–54·5 cm). The blood samples were also obtained from 15 neonates (postnatal day 3–7) whose cord blood had already been collected and the changes in adiponectin concentrations were examined.

MEASUREMENTS The adiponectin concentration was determined by enzyme-linked immunosorbent assay. The leptin concentration was determined by radioimmunoassay. Insulin, GH and IGF-1 concentrations were determined by immunoradiometric assays.

RESULTS The plasma adiponectin concentrations in cord blood ranged from 6·0 to 55·8 μg/ml (median 22·4 μg/ml), which were much higher than those in normal-weight adults ($P < 0·0001$). In contrast to the findings in adults, these values were positively correlated with birth weight ($r = 0·43$, $P = 0·0005$), body mass index ($r = 0·44$, $P = 0·0005$), birth weight/birth length ratio ($r = 0·46$, $P = 0·0002$) and the leptin concentrations ($r = 0·39$, $P = 0·004$). When the effects of fat mass-related anthropometric parameters such as the birth weight/birth length ratio were controlled, plasma adiponectin concentrations had a significant inverse correlation with insulin concentrations ($r = -0·35$, $P = 0·01$). There was no significant gender difference in adiponectin concentrations among newborns. The adiponectin concentrations in neonates (postnatal day 3–7) did not change significantly compared with those in cord blood.

CONCLUSIONS In contrast to the findings in adults, these results suggest that the adiponectin concentration increases with the mass of fetal fat.

Since the discovery of adipocyte-derived hormones, especially leptin (Zhang *et al.*, 1994), adipose tissue has been thought of not only as a means to store fat, but also as a kind of endocrinological organ that secretes a variety of bioactive molecules and regulates whole-body metabolism (Berg *et al.*, 2002). Adiponectin, also known as APM1, Acrp30, or adipoQ, is an adipocyte-derived plasma protein of 244 amino acids that is thought to stimulate glucose utilization and fatty-acid oxidation through the activation of 5′AMP-activated protein kinase (Scherer *et al.*, 1995; Hu *et al.*, 1996; Maeda *et al.*, 1996; Nakano *et al.*, 1996; Yamauchi *et al.*, 2002). Unlike leptin, the plasma adiponectin concentration is inversely correlated with body weight and the amount of fat mass, and this inverse correlation has been suggested to be related to the origin of insulin resistance in obese subjects (Arita *et al.*, 1999; Hotta *et al.*, 2001).

It has been reported that the adiponectin concentration in mice was low in neonates but increased with age (Combs *et al.*, 2003). Adiponectin has also been found in human cord blood (Lindsay *et al.*, 2003). However, its correlation with anthropometric parameters and other hormones have not been fully determined. In newborns, most body fat accumulates in a subcutaneous region, and there is very little visceral fat (Harrington *et al.*, 2002). Adipocytes are smaller than those in adults (Boulton *et al.*, 1978; Soriguer Escofet *et al.*, 1996). Previously we and others examined leptin concentrations in cord blood. Despite differences in the distribution and size of adipocytes, these were both positively correlated with body weight and body mass index (BMI), similar to the findings in adults (Matsuda *et al.*, 1997, 1999; Schubring *et al.*, 1997; Cetin *et al.*, 2000). It is, then, of interest to measure the plasma concentration of adiponectin during the perinatal period, as differences in the distribution and size of adipocytes may affect how its concentration is regulated, and this could provide information regarding the origin of the paradoxical inverse correlation observed in adults.

In the present study, we measured the adiponectin concentration in cord and neonatal blood and examined its relationship with of other hormones and anthropometric parameters.

Correspondence: Ichiro Yokota, MD, Department of Pediatrics, School of Medicine, University of Tokushima, 3-kuramoto cho, Tokushima 770–8503, Japan. Tel: +81-88-633-7135; Fax: +81-88-631-8697. E-mail: yichiro@clin.med.tokushima-u.ac.jp

Table 1 Characteristics of the fetus and plasma adiponectin concentration in cord blood

	Total (n = 59) Median (range)	Male (n = 36) Median (range)	Female (n = 23) Median (range)
Gestational week	39·3 (37·0–41·4)	39·4 (37·0–41·3)	39·0 (37·0–41·4)
Birth weight (g)	2972 (2146–4326)	2994 (2206–3778)	2840 (2146–4326)
Birth length (cm)	48·5 (44·0–54·5)	48·4 (44·0–52·5)	48·0 (44·0–54·5)
Body mass index (kg/m^2)	12·7 (10·1–15·3)	12·8 (10·6–15·3)	12·5 (10·1–15·3)
Birth weight/Birth length (g/cm)	60·8 (46·7–79·4)	61·5 (49·0–74·1)	60·4 (46·7–79·4)
Placental weight (g)	528·0 (322–804)	509·5 (325–804)	562·0 (322–783)
Adiponectin (μg/ml)	22·4 (6·0–55·8)	22·6 (6·0–55·8)	22·0 (17·0–35·8)

Subjects and methods

Subjects

Venous cord blood samples were obtained from 59 full-term healthy newborns (36 males and 23 females, gestational age 37·0–41·4 weeks, birth weight 2146–4326 g, birth length 44·0–54·5 cm; Table 1) Blood samples for adiponectin assay were collected in chilled tubes containing EDTA.2Na (1 mg/ml) and aprotinin (500 U/ml), and plasma was separated at 4 °C immediately after birth. Serum was simultaneously separated for other hormone assays. Neonatal venous blood samples were obtained from 15 full-term healthy neonates (seven males and eight females, postnatal day 3–7), whose cord blood had already been collected, and the difference in the adiponectin concentration between cord and neonatal blood was examined. Each neonatal sample was collected before the subject was fed milk. Plasma samples from nonobese nondiabetic adults (eight males and nine females, age 23–50 years, BMI 17·6–24·0) were also collected after an overnight fast.

Plasma and serum samples were kept frozen at −80 °C until analysis. All of the newborns and neonates were healthy and born at our hospital by normal delivery. Their mothers had had no specific complications, such as gestational diabetes, during pregnancy. The study protocol was approved by the ethics committee of The University of Tokushima, School of Medicine, and all of the parents of the newborns gave their written informed consent before enrolment.

Assays of adiponectin and other hormones

The plasma adiponectin concentration was determined by an enzyme-linked immunosorbent assay (ELISA) using an ELISA kit (Otsuka Assay Institute, Tokushima, Japan; Arita *et al.*, 1999; Matsubara *et al.*, 2003). Serum leptin was determined using an RIA kit (Linco Research, Inc., St Charles, MO, USA). Serum immunoreactive insulin (IRI) was determined using an immunoradiometric assay kit (Eiken Chemical, Tokyo, Japan). Serum GH and IGF-1 were determined using immunoradiometric assay kits (Daiichi Radioisotope Laboratories, Tokyo, Japan).

Statistical analysis

All quantitative data are presented as the median and range. Pearson's correlations were used to analyse relationships among anthropometric parameters and hormone levels. Differences between groups were evaluated by the Mann–Whitney U-test or Wilcoxon's signed rank test. Significance was considered to be $P <$ 0·05. The analysis was conducted with StatView software (version 5·0 for Windows, SAS Institute Inc., Cary, NC, USA) or SPSS software (version 11·0 for Windows, SPSS Inc., Chicago, IL, USA).

Results

In 59 cord blood samples, the plasma adiponectin concentrations ranged from 6·0 to 55·8 μg/ml (median 22·4 μg/ml), which were significantly higher than those in 17 nonobese adults (median 8·2 μg/ml, range 3·1–21·3 μg/ml, $P < 0·0001$). No significant gender difference in the adiponectin concentration was observed in cord blood ($P = 0·99$), although there was a significant gender difference in adults ($P = 0·003$; Fig. 1). The adiponectin concentrations were positively correlated with birth weight ($r = 0·43$, $P = 0·0005$), gestational age ($r = 0·35$, $P = 0·01$), BMI ($r = 0·44$, $P = 0·0005$), the birth weight (BW)/birth length (BL) ratio ($r = 0·46$, $P = 0·0002$) and the leptin concentration ($r = 0·39$, $P = 0·004$; Tables 2 and 3 and Fig. 2).

Because each hormonal factor was correlated with fat mass-related anthropometric parameters, we performed some partial correlation analyses to examine the correlation between each hormone while controlling the effects of anthropometric parameters. The partial correlation between adiponectin and leptin, while controlling for birth weight, BMI or BW/BL ratio, showed a reduced statistical significance ($r = 0·23$, 0·24, 0·20 and $P = 0·11$, 0·09, 0·15, respectively). On the other hand, while controlling for these anthropometric parameters, adiponectin and

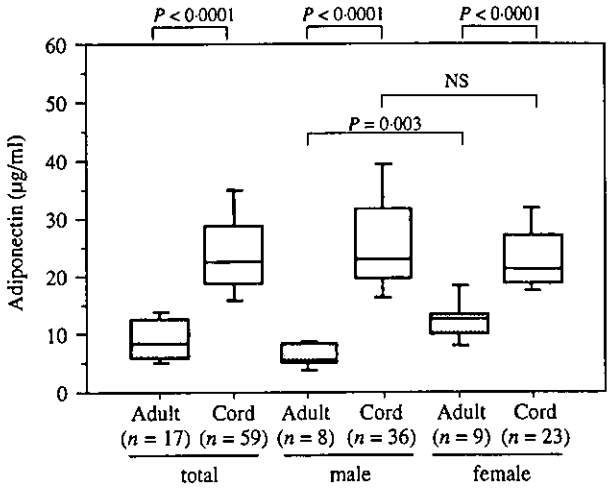

Fig. 1 Comparison of plasma adiponectin concentrations in newborns and nonobese adults. Open rectangles and bars show the results in cord blood and shaded rectangles and bars show those in nonobese adults. The rectangles and bars show the range of the 75th and 90th percentile values, respectively. The horizontal line in each rectangle indicates the median value. ns, not significant.

Table 2 Correlation coefficients between anthropometric parameters and cord blood hormone levels

	Adiponectin	Leptin	Insulin	GH	IGF-1
Birth weight	0·43†	0·49*	0·34‡	−0·47*	0·30‡
Birth length	0·22	0·24	0·26	−0·41†	0·09
BMI	0·44†	0·46†	0·24	−0·30‡	0·38†
BW/BL	0·46*	0·51*	0·32‡	−0·44†	0·36‡
Placental weight	0·18	0·25	0·16	−0·44†	0·43†

*$P < 0·0005$, †$P < 0·005$, ‡$P < 0·05$.

Table 3 Correlation coefficients between cord blood hormone levels

	Adiponectin	Leptin	Insulin	GH
Leptin	0·39†			
Insulin	−0·15	0·01		
GH	−0·21	−0·15	−0·27	
IGF-1	0·10	0·15	0·21	−0·47*

*$P < 0·0005$, †$P < 0·005$.

insulin showed a significant inverse correlation ($r = -0·34$, $-0·28$, $-0·35$ and $P = 0·01$, $0·04$, $0·01$, respectively).

The partial correlation between adiponectin and gestational week controlled for birth weight showed diminished statistical significance ($r = 0·26$, $P = 0·07$). On the other hand, that between adiponectin and birth weight when controlled for gestational week remained significant ($r = 0·31$, $P = 0·03$).

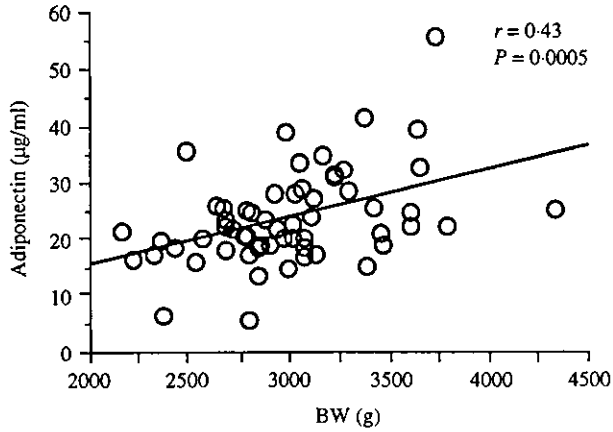

Fig. 2 Correlations between the plasma adiponectin concentration and birth weight. Significant positive correlations were seen between the adiponectin concentration in cord blood and birth weight. The solid line is the regression line.

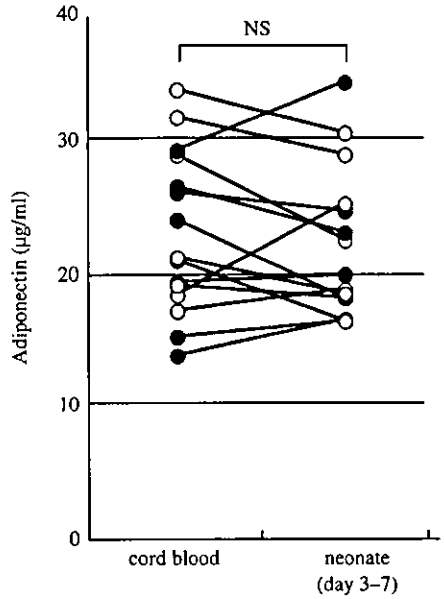

Fig. 3 Changes in the plasma adiponectin concentration after birth. The plasma adiponectin concentrations at birth (cord blood) and in the early neonatal period (postnatal days 3–7) were compared in 15 newborns (seven males, eight females). Each bar shows the change in the adiponectin concentration in each newborn; ●, male; ○, female. The adiponectin concentrations did not change significantly during this period.

In 15 neonates, the plasma adiponectin concentrations ranged from 16·3 to 34·3 μg/ml (median 19·8 μg/ml). In contrast to the leptin concentration, which showed a significant decrease during the early neonatal period (Matsuda *et al.*, 1999), the plasma adiponectin concentration did not change significantly compared with those in newborns ($P = 0·32$; Fig. 3). There was no significant

difference in the adiponectin concentration between males ($n = 7$, median 19·8 μg/ml, range 16·3–34·3 μg/ml) and females ($n = 8$, median 20·6 μg/ml, range 16·3–30·5 μg/ml; $P = 0·73$).

Discussion

Our results showed that the fetal and neonatal adiponectin concentrations are higher than those in adults and correlated positively with fat mass-related anthropometric parameters. This high concentration of adiponectin is inconsistent with a finding in mice of a significantly low level of adiponectin at 1 week of age (Combs *et al.*, 2003), although low fat mass volume in mice during this period should be taken into consideration. The positive correlations are completely opposite those reported in adult humans (Arita *et al.*, 1999), but are consistent with a previous report that found positive correlation between subscapular skin thickness of neonates and cord adiponectin concentrations (Lindsay *et al.*, 2003).

The percentage of total body fat in full-term newborns has been reported to be around 15% using different methods such as anthropometric and skin-fold measurements, chemical dissection, dual-energy X-ray absorptiometry and magnetic resonance imaging (MRI; Forsum & Sadurskis, 1986; White *et al.*, 1991; Picaud *et al.*, 1996; Harrington *et al.*, 2002). An MRI study in full-term newborns showed that nearly 90% of adipose tissue exists in the subcutaneous region, whereas only 4% exists in the visceral region (Harrington *et al.*, 2002). Preadipocytes begin to differentiate into small adipocytes (fewer than 25 microns in diameter) *in utero* and most adipocytes are of this type at birth (Boulton *et al.*, 1978). The increase in the fat mass volume during the last 2 months of fetal life depends on fat cell replication (Enzi *et al.*, 1981). Although we did not measure fat cell size, adipose mass or the regional distribution of adipose tissues in our subjects, good correlations have been found between body fat content and these anthropometric parameters, especially the BW/BL ratio in newborns (Wolfe *et al.*, 1990). Thus, this result suggests that the increased amount of fat mass together with the increased number of small adipocytes which mostly exist in the subcutaneous region increases the adiponectin production in humans. In adults, the secretion of adiponectin by omental cells has been shown to have a strong negative correlation with BMI (Motoshima *et al.*, 2002). In addition, the intra-abdominal fat area by CT scan was negatively correlated with the adiponectin concentration (Cnop *et al.*, 2003). Thus, the very low percentage of visceral fat in newborns may somehow be related to our result. The positive correlation between gestational age and adiponectin concentration in our study raises the possibility that the difference in gestational age reflects the positive correlation between fat mass and adiponectin concentration. However, our partial correlation analysis suggests that adiposity, not gestational age, is predominantly correlated with the adiponectin concentration.

Expression of the adiponectin gene is modulated by many factors *in vitro*. The adiponectin mRNA level has been shown to be increased by insulin and IGF-1, but decreased by tumour necrosis factor (TNF)-α, plasminogen activator inhibitor (PAI)-1, interleukin (IL)-6 and glucocorticoid (Halleux *et al.*, 2001; Fasshauer *et al.*, 2003; Kern *et al.*, 2003). Positive correlations have been reported between birth weight and both IGF-1 and insulin (Ong *et al.*, 2000), and these were also observed in this study. Thus, the effects of these factors on the correlation between birth weight and the adiponectin concentration might also be taken into consideration.

During childhood, the plasma adiponectin concentration has been reported to be negatively correlated with the percentage of body fat at 5 years of age and to decrease with increasing adiposity longitudinally (Stefan *et al.*, 2002). This result suggests that the relationship between adiposity and the adiponectin concentration may change from positive to negative during early childhood. After birth, the size of adipocytes rapidly increases during the first 6 months of life, slightly decreases over the second 6 months, and then increases slowly (Soriguer Escofet *et al.*, 1996). The percentage of visceral fat has been reported to increase to about 11% of the total fat mass in nonobese prepubertal (4·4–8·8 years old) children (Goran *et al.*, 1995). Thus, the longitudinal changes in this correlation may be explained by the changes in the distribution and size of adipocytes during this period.

The high concentration of adiponectin and its positive correlation with birth weight raises a question regarding its physiological action during the neonatal period. It is known that neonates are more sensitive to insulin than adults (Farrag *et al.*, 1997), which might be consistent with a high adiponectin concentration at birth. With regard to insulin sensitivity, one author reported that low birth weight neonates had increased insulin resistance (Gray *et al.*, 2002), whereas others reported that small for gestational age infants had increased insulin sensitivity with respect to glucose disposal but not to the suppression of lipolysis, ketogenesis, or the hepatic suppression of IGFBP-1 (Bazaes *et al.*, 2003; Soto *et al.*, 2003). Thus, we cannot fully associate the positive correlation between the adiponectin concentration and birth weight with insulin sensitivity.

In cord blood, both adiponectin and insulin are positively correlated with fat mass-related anthropometric parameters. However, the negative correlation between adiponectin and insulin, while controlling for these parameters, suggests that their secretion is regulated in a different manner under the same adiposity. In other words, something except the mass of fetal fat may cause this negative correlation. In adults, a negative correlation has been observed between the adiponectin concentration and the calculated insulin resistance [homeostasis model assessment ratio (HOMA-R)] independent of adiposity (Matsubara *et al.*, 2003). It is possible that the negative correlation between

adiponectin and insulin in cord blood, while controlling for fat mass-related anthropometric parameters, may suggest a similar relation if the cord blood insulin concentration can be assumed to reflect insulin sensitivity. Alternatively, this negative correlation might be explained by the stimulation of IL-6 and TNF-α by insulin, as observed in adult subcutaneous adipose tissue (Krogh-Madsen *et al.*, 2003), which would lead to an inhibition of adiponectin secretion.

In adults, there is an apparent gender difference in the plasma adiponectin concentration, i.e. males have significantly lower adiponectin concentrations than females. It is possible that this difference originates in the difference in the testosterone level, which decreases the plasma adiponectin concentration through its effect on the secretion of adiponectin from adipocytes (Nishizawa *et al.*, 2002). However, the effect of castration in male mice or rats is controversial (Nishizawa *et al.*, 2002; Combs *et al.*, 2003). In newborns, no significant gender difference was observed. In the male fetus, the testosterone level increases from the end of the second month of gestation, soon reaches a maximal value that is maintained until late in gestation and then decreases. At birth, testosterone levels in males are higher than those in females. Thus, the exposure to testosterone *in utero* does not influence the adiponectin level at birth. In rats, while exposure to testosterone during the perinatal period also does not alter the adiponectin level at that time, it may influence its level in adulthood, as castration of the testes during the early neonatal period feminized its level in the adult male (Combs *et al.*, 2003). The adiponectin level in humans with sex-independent perinatal androgen levels, such as females with congenital adrenal hyperplasia or males with congenital hypothalamic hypogonadism, may provide information regarding the role of perinatal androgen exposure to the regulation of adiponectin production in humans.

In summary, this study has demonstrated the existence of adiponectin in fetal and neonatal blood at high concentrations, positive correlations between the cord blood adiponectin concentration and fetal fat mass-related parameters, and an absence of a gender difference in the adiponectin concentration at birth. The positive relationship with fat mass-related parameters seen during this period might reflect differences in adipocyte size and body fat distribution in the newborn *vs.* the adult.

Acknowledgements

We thank Dr K. Maeda and Prof M. Irahara (Department of Obstetrics & Gynecology, School of Medicine, University of Tokushima) for their support with the sample collection.

References

Arita, Y., Kihara, S., Ouchi, N., Takahashi, M., Maeda, K., Miyagawa, J., Hotta, K., Shimomura, I., Nakamura, T., Miyaoka, K., Kuriyama, H., Nishida, M., Yamashita, S., Okubo, K., Matsubara, K., Muraguchi, M., Ohmoto, Y., Funahashi, T. & Matsuzawa, Y. (1999) Paradoxical decrease of an adipose-specific protein, adiponectin, in obesity. *Biochemistry and Biophysics Research Communications*, **257**, 79–83.

Bazaes, R.A., Salazar, T.E., Pittaluga, E., Pena, V., Alegria, A., Iniguez, G., Ong, K.K., Dunger, D.B. & Mericq, M.V. (2003) Glucose and lipid metabolism in small for gestational age infants at 48 hours of age. *Pediatrics*, **111**, 804–809.

Berg, A.H., Combs, T.P. & Scherer, P.E. (2002) ACRP30/adiponectin: an adipokine regulating glucose and lipid metabolism. *Trends in Endocrinology and Metabolism*, **13**, 84–89.

Boulton. T.J., Dunlop, M. & Court, J.M. (1978) The growth and development of fat cells in infancy. *Pediatric Research*, **12**, 908–911.

Cetin, I., Morpurgo, P.S., Radaelli, T., Taricco, E., Cortelazzi, D., Bellotti, M., Pardi, G. & Beck-Peccoz, P. (2000) Fetal plasma leptin concentrations: relationship with different intrauterine growth patterns from 19 weeks to term. *Pediatric Research*, **48**, 646–651.

Cnop, M., Havel, P.J., Utzschneider, K.M., Carr, D.B., Sinha, M.K., Boyko, E.J., Retzlaff, B.M., Knopp, R.H., Brunzell, J.D. & Kahn, S.E. (2003) Relationship of adiponectin to body fat distribution, insulin sensitivity and plasma lipoproteins: evidence for independent roles of age and sex. *Diabetologia*, **46**, 459–469.

Combs, T.P., Berg, A.H., Rajala, M.W., Klebanov, S., Iyenga, R.P., Jimenez-Chillaron, J.C., Patti, M.E., Klein, S.L., Weinstein, R.S. & Scherer, P.E. (2003) Sexual differentiation, pregnancy, calorie restriction, and aging affect the adipocyte-specific secretory protein adiponectin. *Diabetes*, **52**, 268–276.

Enzi, G., Zanardo, V., Caretta, F., Inelmen, E.M. & Rubaltelli, F. (1981) Intrauterine growth and adipose tissue development. *American Journal of Clinical Nutrition*, **34**, 1785–1790.

Farrag, H.M., Nawrath, L.M., Healey, J.E., Dorcus, E.J., Rapoza, R.E., Oh, W. & Cowett, R.M. (1997) Persistent glucose production and greater peripheral sensitivity to insulin in the neonate *vs.* the adult. *American Journal of Physiology*, **272**, E86–E93.

Fasshauer, M., Kralisch, S., Klier, M., Lossner, U., Bluher, M., Klein, J. & Paschke, R. (2003) Adiponectin gene expression and secretion is inhibited by interleukin-6 in 3T3-L1 adipocytes. *Biochemical and Biophysical Research Communications*, **301**, 1045–1050.

Forsum, E. & Sadurskis, A. (1986) Growth, body composition and breast milk intake of Swedish infants during early life. *Early Human and Development*, **14**, 121–129.

Goran, M.I., Kaskoun, M. & Shuman. W.P. (1995) Intra-abdominal adipose tissue in young children. *International Journal of Obes*, **19**, 279–283.

Gray, I.P., Cooper, P.A., Cory, B.J., Toman, M. & Crowther, N.J. (2002) The intrauterine environment is a strong determinant of glucose tolerance during the neonatal period, even in prematurity. *Journal of Clinical Endocrinology and Metabolism*, **87**, 4252–4256.

Halleux, C.M., Takahashi, M., Delporte, M.L., Detry, R., Funahashi, T., Matsuzawa, Y. & Brichard, S.M. (2002) Secretion of adiponectin and regulation of apM1 gene expression in human visceral adipose tissue. *Biochemical and Biophysical Research Communications*, **288**, 1102–1107.

Harrington, T.A., Thomas, E.L., Modi, N., Frost, G., Coutts, G.A. & Bell, J.D. (2002) Fast and reproducible method for the direct quantitation of adipose tissue in newborn infants. *Lipids*, **37**, 95–100.

Hotta, K., Funahashi, T., Bodkin, N.L., Ortmeyer, H.K., Arita, Y., Hansen, B.C. & Matsuzawa, Y. (2001) Circulating concentrations of the adipocyte protein adiponectin are decreased in parallel with reduced insulin sensitivity during the progression to type 2 diabetes in rhesus monkeys. *Diabetes*, **50**, 1126–1133.

